5/8-25

1996

NASA/ASEE SUMMER FACULTY FELLOWSHIP PROGRAM

MARSHALL SPACE FLIGHT CENTER
THE UNIVERSITY OF ALABAMA

# THERMAL MODEL OF THE PROMOTED COMBUSTION TEST

Prepared By: Peter D. Jones, Ph.D., P.E.

Academic Rank: Associate Professor

Institution and Department: Auburn University
Mechanical Engineering Department

NASA/MSFC:

Laboratory: Materials and Processes
Division: Metallic Materials and Processes
Branch: Metallurgical Research and Development

MSFC Colleague: Biliyar N. Bhat, Ph.D.

## INTRODUCTION

Flammability of metals in high pressure, pure oxygen environments, such as rocket engine turbopumps, is commonly evaluated using the Promoted Combustion Test (PCT). The PCT emphasizes the ability of an ignited material to sustain combustion, as opposed to evaluating the sample's propensity to ignite in the first place. A common arrangement is a rod of the sample material hanging in a chamber in which a high pressure, pure oxygen environment is maintained. An igniter of some energetically combusting material is fixed to the bottom of the rod and fired. This initiates combustion, and the sample burns and melts at its bottom tip. A ball of molten material forms, and this ball detaches when it grows too large to be supported by surface tension with the rod. In materials which do not sustain combustion, the combustion then extinguishes. In materials which do sustain combustion, combustion re-initiates from molten residue left on the bottom of the rod, and the melt ball burns and grows until it detaches again.

The purpose of this work is development of a PCT thermal simulation model, detailing phase change, melt detachment, and the several heat transfer modes. Combustion is modeled by a summary rate equation, whose parameters are identified by comparison to PCT results. The sensitivity of PCT results to various physical and geometrical parameters is evaluated. The identified combustion parameters may be used in design of new PCT arrangements, as might be used for flammability assessment in flow-dominated environments.

The Haynes 214 nickel-based superalloy, whose PCT results are applied here, burns heterogeneously (fuel and oxidizer are of different phases; combustion takes place on the fuel surface). Heterogeneous combustion is not well understood. (In homogeneous combustion, the metal vaporizes, and combustion takes place in an analytically treatable cloud above the surface). Thermal modeling in heterogeneous combustion settings provides a means for linking test results more directly to detailed combustion mechanics, leading to improved data analysis, and improved understanding of heterogeneous combustion phenomena.

## ANALYSIS

The vertical rod, bottom ignited arrangement for PCT is divided into liquid and solid zones (an intermediate mushy zone, appropriate for alloys, could be considered as an extension). Heat transfer in the solid is one-dimensional along the rod axis. Heat transfer in the liquid is ideally two-dimensional (symmetric about the rod axis) and coupled to the flow field arising from introduction of new material at the phase interface (solid consumption), surface tension and gravity defining the liquid surface geometry, and combustion mass transfer on the surface. However, the liquid zone is approximated as quasi-one-dimensional. in order to pursue the simplest possible descriptive model of PCT thermal transport, viz:

$$A_l(x) = \pi(x^2 + r^2), \quad V_l(x) = \frac{\rho_s A_s V_s}{\rho_l A_l(x)}, \quad \frac{dl_x}{dt} = V_l(l_x), \quad m_l = \rho_l \frac{\pi l_x}{6}(l_x^2 + 3r^2). \qquad (1)$$

The liquid surface is modeled as a sphere truncated by the rod end (Fig.1). As the molten ball grows, its shape changes from an thin spherical cap, through the shape of a hemisphere.

and continues to the shape of a sphere minus a spherical cap. The velocity field accounts for mass flux continuity with the rod consumption. Velocity is considered constant over, and normal to, spherical surfaces defined by $x$. When the weight of the liquid exceeds surface tension, the liquid detaches, and $l_x$ reverts to a residue $l_{x,o}$. Whether combustion continues at that point depends on the temperature distribution within $l_{x,o}$ and the magnitude of the linear consumption rate, $V_s$. These quantities are determined here by means of transient, multiphase, combined mode heat transfer analysis of the simplified geometry defined above.

Combustion heat generation on the liquid surface is in equilibrium with conduction to the liquid, radiation to the chamber, natural convection, and transient effects. Conduction through the liquid carries heat to the phase boundary, where it is dissipated by the heat of fusion, conduction up the rod, radiation from the rod to the chamber, and transient effects. The rod is in the natural convection flow generated by the molten ball, and so convective transfer is directed into the rod. These effects are represented by the phase-separated model:

$$\rho_s c_s A_s \left[ \frac{\partial T_s}{\partial t} + (S-1)\frac{V_s}{l_s}\frac{\partial T_s}{\partial S} \right] = \frac{k_s A_s}{l_s^2}\frac{\partial^2 T_s}{\partial S^2} - P_s h_s (T_s - T_\infty) - P_s \epsilon_s \sigma_b (T_s^4 - T_w^4) \qquad (2)$$

in the solid zone and

$$\rho_l c_l A_l \left[ \frac{\partial T_l}{\partial t} + (1-X)\frac{V_l}{l_x}\frac{\partial T_l}{\partial X} \right] = \frac{k_l}{l_x^2}\left( A_l \frac{\partial^2 T_l}{\partial X^2} + \frac{\partial A_l}{\partial X}\frac{\partial T_l}{\partial X} \right) \qquad (3)$$

in the liquid zone, with boundary conditions of an adiabatic tip at $s=l_s$,

$$T_s|_{S=0} = T_m = T_l|_{X=0}, \quad \rho_s V_s h_{sl} = \left.\frac{k_s}{l_s}\frac{\partial T_s}{\partial S}\right|_{S=0} + \left.\frac{k_l}{l_x}\frac{\partial T_l}{\partial X}\right|_{X=0} \qquad (4)$$

at the phase boundary, and

$$\Delta H_c C \left(\frac{p}{p_{ref}}\right)^a \exp\left(\frac{-E_c}{R T_l|_{X=1}}\right) = \left.\frac{k_l}{l_x}\frac{\partial T_l}{\partial X}\right|_{X=1} + h_l\left(T_l|_{X=1} - T_w\right) + \sigma_b\left(T_l|_{X=1}^4 - T_w^4\right) \qquad (5)$$

on the liquid surface. The origin of $s$ and $x$ is fixed at the moving phase interface, and these coordinates are made dimensionless by $s=Sl_s$ and $x=Xl_x$. The coordinates are both moving and stretching, so the von Mises time transformation is applied. The combustion model is a summary rate equation governed by oxidizer transport through an oxide layer forming on the liquid. This rate is considered time-independent, though oxide thickness increases in an amount limited by stretching of the molten ball until it detaches and the layer re-initiates. The rate is considered uniform over the surface, as no bright spots or lines are observed in PCT data for the material considered (Haynes 214). The liquid convection coefficient is approximated as natural convection from a sphere. The free stream temperature is modeled as a spreading plume from a point source of strength equal to the convection from the liquid. The solid convection coefficient is defined by flow over an axisymmetric blunt body.

The model is solved numerically. Combustion and radiation terms and temperature-

dependent coefficients are linearized. The structure is iterative-tridiagonal within a time step. Convergence takes less than ten iterations, and over/under-relaxation is not necessary. Central difference conductive terms are used, though upwinding is necessary for convective terms, giving the algorithm spatial first order accuracy. The Crank-Nicholson scheme (second order accurate) is used for marching in time. Time instabilities are encountered and traced to interaction between combustion and radiation terms. It is necessary to lag the combustion temperature by several time steps. A more stable coupling must be developed analytically to avoid recourse to this device. Although the liquid radiative flux is small, it plays a vital limiting role. Temperature diverges if liquid surface radiation is neglected.

The model is sensitive to many parameters which are only approximately known (thermophysical properties of molten metal), or completely unknown (constants in the combustion rate expression). To estimate the combustion parameters, the model is solved analytically, neglecting transience, convection, radiation, and finite rod length, resulting in:

$$\Delta H_c C\left(\frac{p}{p_{ref}}\right)^a \exp\left(\frac{-E_c}{RT_{ig}}\right) = \rho_s V_s\left[h_{sl}+c_s(T_m-T_w)\right]\exp\left\{\frac{A_s V_s}{\pi\alpha_s r}\tan^{-1}\left(\frac{l_x}{r}\right)-\left(1+\frac{A_s V_s}{\pi\alpha_s x}\right)\ln\left[1+\left(\frac{l_x}{r}\right)^2\right]\right\} \quad (6)$$

where $T_{ig}$ is an effective ignition temperature. The heat of combustion (left side of Eq.(6)) is related to the linear consumption rate, $V_s$. This is determined from video recordings of PCT runs, stepping through frame by frame and measuring the amount of consumption (as a ratio of the rod diameter) between detachments. (A flame corona obscures the phase interface at all other times). 33 PCT recordings for Haynes 214 at six pressures between 7 and 69 MPa were examined. The results of $V_s$ vs. $p$ are shown in Fig.2. A power law function of pressure is chosen to fit the observed consumption rate, with the result

$$V_s = 4.944\frac{mm}{s}\left(\frac{p}{p_{ref}}\right)^{0.06744} \quad (7)$$

where $p_{ref}$=1 MPa. For this slight pressure dependence, the exponential terms in the right side of Eq.(6) have little influence, and the pressure exponent $a$ is given the experimentally determined value 0.06744. Using $T_{ig}$=3000 K, $E_c=3\times10^5$ J/gmol, $\Delta H_c=7.64\times10^6$ J/kg and $h_{sl}=1.5\times10^5$ J/kg, the reaction rate preconstant $C=6.6\times10^5$ kg/m$^2$s is determined. Although this value is sensitive to the $T_{ig}$ guess, it serves as a starting point for identification using the full model. Full model identification yields $C=5.0\times10^5$ kg/m$^2$s.

## RESULTS

Figure 3 shows the surface temperature history of the liquid for a base case, with a chamber pressure of 7 MPa (1000 psi), and a high pressure case at 69 MPa (10,000 psi). Figure 4 shows the linear consumption rate history. Applying the igniter energy to melt a volume of the rod and bring it to $T_{ig}$ defines the initial state. Choice of $T_{ig}$ is found to have very little effect after the first detachment. Base case interdetachment time is observed to be 0.5 s, and the unknown surface tension is adjusted to normalize the simulation. Surface temperature rises after detachment; faster at first, then slower as the ball grows and more of the heat of combustion goes into heating the liquid, with a total temperature rise of 400 K

(720°F) before detachment. High pressure case behavior is similar, except that it burns 200 K (360°F) hotter and detaches 0.04 s sooner. Consumption rate levels off after the first detachment, with a slight loss at each subsequent detachment. The high pressure case has a slightly higher consumption rate than the base case, as it burns hotter, has a hotter residue, and hence is more likely to maintain combustion than the base case.

Figures 5 and 6 show the effect of altering the diameter of the PCT article from the base case (3.2 mm or ⅛ in.) to a thin case of (1.6 mm or $^1/_{16}$ in.). The thin case shows a longer interdetachment time and a larger temperature increase within one drop. It has twice the linear consumption rate (mm/s, half the volumetric consumption rate, $mm^3/s$) of the base case. The surface tension-based drop detachment model allows a maximum drop volume which is roughly proportional to rod diameter. Since the thin case has half the surface tension perimeter of the base case, the interdetachment time might therefore be expected to be the same. However, the molten residue length has been modeled as a constant multiple of the rod diameter. Therefore, in the thin case, the new drop starts out much smaller and cooler after detachment than in the base case. Behavior very similar to that of the thin case is also found for the base case if the residue multiplier is halved. Clearly, the modeling of detachment and residue phenomena has a significant impact on PCT simulation results.

Other PCT parameters considered are: rod length and initial temperature; chamber temperature; and igniter energy. A short case (15.2 cm or 6 in. - base case is 30.5 cm or 12 in.) has results which cannot be distinguished from the base case, indicating that the cold end boundary condition has no effect. A hot case with an initial temperature of 500 K (440°F - base case is 300 K or 80°F) is also indistinguishable from the base case indicating that the high combustion temperatures dominate any uncertainty in test article initial conditions. A hot chamber case ($T_w$=500 K or 440°F - base case is 300 K or 80°F) shows no differences. Varying igniter energy ±10% has no effect beyond first detachment. However, the speed and temperature with which this point is reached are sensitive to igniter energy.

## CONCLUSIONS

Vertical rod, bottom ignited PCT arrangements are simulated. Simulation is sensitive to: modeling of drop detachment and residue phenomena; numerical stability of combustion and radiation interaction; and thermophysical properties of liquid metals for which data is sparse. Clarification of these issues will result in a more accurate simulation, which may be applied to the available PCT data to better identify heterogeneous combustion models.

The vertical rod, bottom ignited PCT is fairly insensitive to chamber pressure. This is demonstrated by a simplified solution linking combustion oxidizer mass flow rate to solid consumption rate, and by PCT data showing consumption rate to depend weakly on pressure.

The vertical rod, bottom ignited PCT is fairly insensitive to ignition conditions. Ignition has a strong effect only on the formation of the first molten ball. Subsequent balls are most strongly affected by detachment and residue modeling. Conversely, alternate PCT arrangements not subject to detachment should be more sensitive to ignition conditions. In such cases, a controlled ignition mechanism such as a laser should be considered.

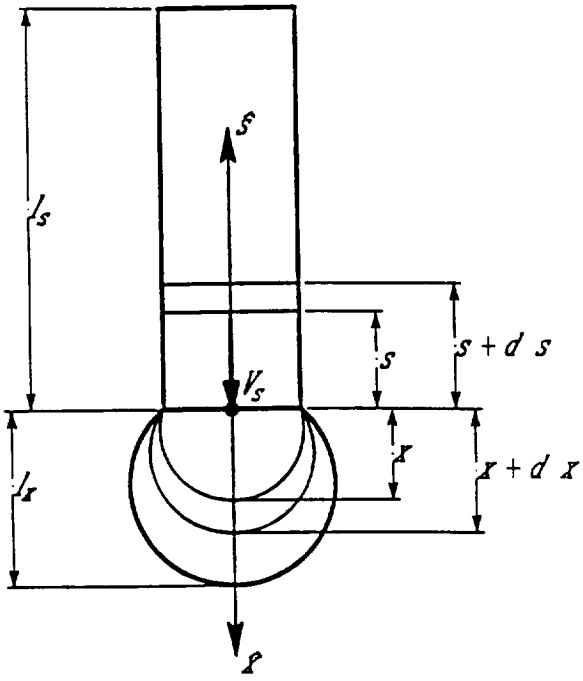


Figure 1 - Coordinate system for vertical rod, bottom ignited PCT

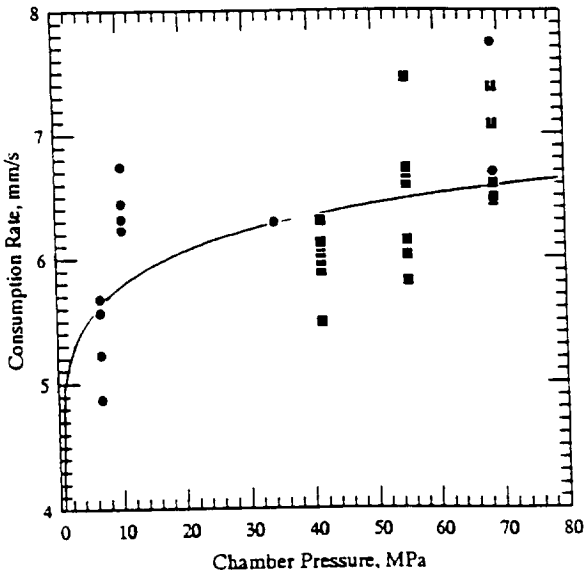


Figure 2 - Linear consumption rate of Haynes 214 - multiple tests at multiple chamber pressures with power law fit

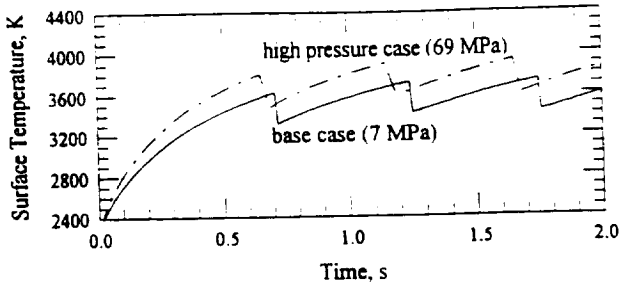


Figure 3 - Surface temperature history for base case and high pressure case

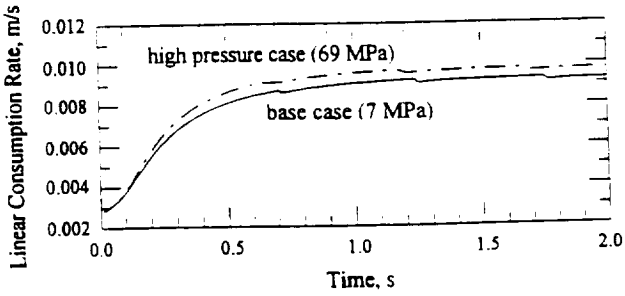


Figure 4 - Linear consumption rate history for base case and high pressure case

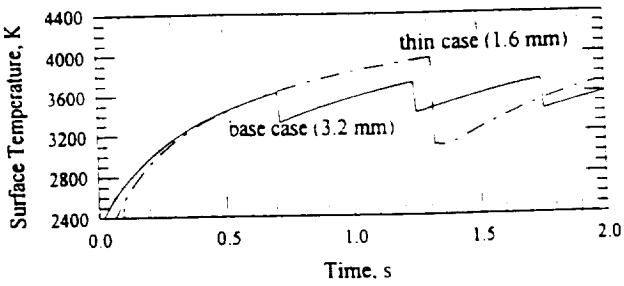


Figure 5 - Surface temperature history for base case and thin rod case

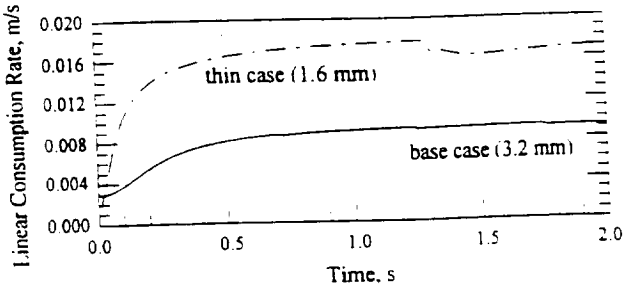


Figure 6 - Linear consumption rate history for base case and thin rod case